BEC of magnons in superfluid ^{3}He-B and symmetry breaking fields

M. Kupka and P. Skyba*

Centre of Low Temperature Physics, Institute of Experimental Physics, SAS and P. J. Šafárik University Košice, Watsonova 47, 04001 Košice, Slovakia

(Received 1 December 2011; revised manuscript received 17 May 2012; published 31 May 2012)

States with a coherent precession of magnetization such as a homogeneously precessing domain or a persistently precessing domain created in the superfluid ^{3}He-B represent the macroscopic examples of the Bose-Einstein condensates of magnons. Once the magnons form one of these states, this many-magnon coherent quantum state is described by a "single-magnon wave function" (or an order parameter). A suitable external perturbation may cause the condensate to oscillate around the state of coherent precession, which demonstrates a collective rigidity of the condensate against scattering a single magnon out of it. The states corresponding to a free coherent precession of magnetization are degenerate in the phase of precession, so there exist oscillations around such states with a gapless dispersion relation, known as the Goldstone modes. Here, we present both experimental and theoretical results of the study of the spin density oscillations superposed on a homogeneously precessing domain in superfluid ^{3}He-B in the presence of a high-frequency excitation field $B_{\rm rf}$. We show that the presence of this field lifts the degeneracy of the precessing state with respect to the phase of precession, that is, it violates the symmetry of the magnon condensate, and former Goldstone modes become non-Goldstone ones, as they acquire the energy gap in their spectrum.

DOI: 10.1103/PhysRevB.85.184529 PACS number(s): 67.30.er, 67.30.hj, 76.60.−k

I. INTRODUCTION

Traditionally, the phenomenon of Bose-Einstein condensation is associated with an ideal Bose gas of identical particles, the number of which is conserved. The condensate is said to be present whenever a finite fraction of all the consistent particles resides in the same lowest single-particle state, all behaving in exactly the same way. During the last several decades, the concept of Bose-Einstein condensation has been extended to various gases of bosonic elementary excitations in many-body systems, that is, the gases of quasiparticles, with finite lifetime, the numbers of which are not conserved.[1] Bose-Einstein condensation in such a gas can only be realized if the lifetime of the quasiparticles considerably exceeds the time they need to scatter with each other to reach thermal equilibrium among themselves. Bose-Einstein condensation of quasiparticles has been reported in several physical systems, such as ensembles of excitons, biexcitons, and polaritons in semiconductors,[2,3] or gases of magnons in certain classes of quantum magnets[4,5] and in superfluid helium-3.[6–9]

With respect to the purpose of the study presented here, i.e., to extend Fomin's work concerning the vibrations of a magnetic domain undergoing free precession to the case when this precession is prescribed by an external rf field, it was more convenient to treat the homogeneously precessing domain (HPD) in ^{3}He-B "classically," that is, in terms of the condensate of Cooper pairs and its order parameter rather than in terms of the condensate of magnons.

Consider a simple pulse NMR experiment. A volume (experimental cell) of superfluid ^{3}He-B is placed in the magnetic field $\mathbf{B}_0$ with linear gradient field ∇B along the z direction ($\mathbf{B} = \mathbf{B}_0 + \nabla B\mathbf{z}$). Steady magnetic field $\mathbf{B}$ induces an equilibrium magnetization, that is, the majority of magnetic momenta are aligned to the field direction. When a perpendicular rf pulse with sufficient amplitude $\mathbf{B}_{\rm rf}$ and a suitable frequency is applied, then the magnetization (spins) in ^{3}He-B is deflected and precesses around the external magnetic field. Inhomogeneity in the external magnetic field forces the differences in frequencies of the spin precession, i.e., it generates the gradients in the spin part of the order parameter. Arising spin supercurrents redistribute the spin deflection over a sample of superfluid ^{3}He-B. A "spin-up" component, i.e., with spins pointing up along the magnetic field, flows towards to lower field, while the "spin-down" component flows towards to the opposite part of the cell, where magnetic field is higher. As both components can not pass through the cell walls, these spin supercurrents have the effect of increasing of the tipping angle at the low-field side of the cell, while reducing it on the other. Thus, the magnetic moments on the high-field side are orientated into the field direction and, once they are parallel, they stop their precession and form a stationary domain (SD). However, the magnetic moments on the low-field side are deflecting until a Leggett angle ($\Theta_L \sim 104^\circ$) is reached, above which the dipole-dipole energy can not be minimized, and this gives rise to a dipole torque. The dipole torque increases the frequency of the spin precession and thus lowers the gradients in the order parameter created due to field gradient and field inhomogeneity. Thus, a dynamic equilibrium state is spontaneously set up, where in a localized volume the spins are precessing coherently in spite of the presence of inhomogeneous magnetic field forming the B-E condensate of magnons: homogeneously precessing domain. The precessing domain and the stationary domain are separated by a domain wall, which concentrates the gradient energy of the system. Position of the domain wall is determined by the condition that the local Larmor frequency at the domain-wall position equals to the frequency of the coherently precessing domain.

Once such a two-domain structure is created, it represents a stable configuration. If this structure is slightly perturbed, it will undergo small oscillations around the homogeneously precessing state. As the states of a free homogeneous precession are degenerate in the phase of precession, there are oscillations with a gapless spectrum in the long-wavelength

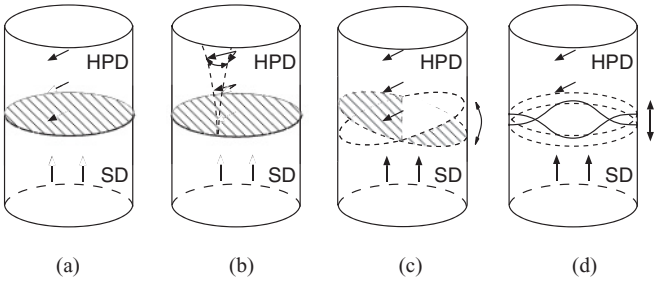

FIG. 1. A schematic visualization of various kinds of the normal modes of an oscillating HPD-SD structure: (a) the HPD-SD stable state, (b) the torsion oscillation mode, (c) the planar mode, and (d) the first axial surface mode.

limit known as the Goldstone modes. There were a variety of the gapless oscillation modes found on the background of a freely precessing two-domain structure. However, if another external field simultaneously lifts this degeneracy of the precessing states, the symmetry violation may be associated with a creation of the energy gap in the spectrum of excitations, and the Goldstone modes become non-Goldstone ones.

The aim of this article is to present both experimental and theoretical results of the study of the oscillation modes of the precessing two-domain structure in superfluid ^{3}He-B in the presence of the symmetry breaking high-frequency excitation field $B_{\rm rf}$.

II. THEORETICAL RESULTS

There are a variety of oscillation modes that can be excited on the background of the dynamic two-domain structure as shown in Fig. 1. In principle, these modes can be divided into two types. While the first one, the so-called twisting oscillations, represent "phonons in the magnon superfluid," the second type is represented by vibrations of the domain wall itself. The latter are in some aspects analogous to those excited on the surface of the liquids in the gravitational field. The above-mentioned oscillation modes superposed on the freely precessing HPD-SD structure were theoretically studied by Fomin,[10–12] and some of them had already been experimentally observed: the torsion oscillation mode and the planar mode using the pulse NMR technique by the Moscow group,[13–15] and the axial mode using the continuous NMR technique by the Košice group.[16,17]

According to Fomin's theory,[12] the frequency of the torsion wave propagating in the HPD volume along the magnetic field reads as

$$\Omega^2 = \frac{2\Omega_B^2}{8\Omega_B^2 + 3\omega_L^2}\left(5c_T^2 - c_L^2\right)k_L^2. \tag{1}$$

Here, k_L is the corresponding wave vector, $\Omega_B(T)$ is the Leggett frequency, c_T and c_L denote the spin-wave velocities with respect to the direction of the magnetic field, and ω_L is the local Larmor frequency at the domain-wall position, that is, the frequency of the coherent spin precession. The dispersion relation of the wave traveling along the HPD-SD interface (surface mode) was found in the form[12]

$$\Omega^2 = \frac{1}{2\sqrt{2}}\frac{\nabla\omega_L}{\omega_L}\sqrt{\left(5c_T^2 - c_L^2\right)\left(5c_L^2 + 3c_T^2\right)}\,k_T\,. \tag{2}$$

Here, k_T is the transverse wave vector and $\nabla\omega_L$ is the small gradient in the Larmor frequency due to a gradient in the applied magnetic field ∇B.

The above-mentioned Fomin's theoretical results were obtained for a two-domain structure undergoing free precession, i.e., in the absence of the external forces. This corresponds to the condition of the HPD excited by a pulse NMR technique. Then, there is the degeneracy of the precessing states with respect to the phase of precession present. However, in the case of a continuous NMR, the high-frequency excitation field $\mathbf{B}_{\rm rf}$ rotating at an angular frequency $\omega_{\rm rf}$ in the plane perpendicular to the direction of static magnetic field $\mathbf{B}$ defines a preference orientation removing thus the U(1) degeneracy of the precessing states. As a result, the dispersion relations of the excitations of a precessing two-domain structure in the long-wavelength region acquire a gap (see the Appendix). Thus, the dispersion relations of the torsion wave traveling in the volume of HPD were obtained in the form

$$\Omega^2 = \frac{3\Omega_B^2}{8\Omega_B^2 + 3\omega_{\rm rf}^2}\left(\frac{4}{\sqrt{15}}g B_{\rm rf}\omega_{\rm rf} + \frac{2}{3}\left(5c_T^2 - c_L^2\right)k_L^2 + \frac{1}{3}\left(5c_L^2 + 3c_T^2\right)k_T^2\right), \tag{3}$$

and that for the wave propagating along the HPD-SD interface was derived in the form

$$\Omega^2 = \frac{3}{4}\frac{g\nabla B}{\omega_{\rm rf}}\sqrt{\frac{2}{3}\left(5c_T^2 - c_L^2\right)} \times\sqrt{\frac{4}{\sqrt{15}}g B_{\rm rf}\omega_{\rm rf} + \frac{1}{3}\left(5c_L^2 + 3c_T^2\right)k_T^2}\,. \tag{4}$$

Here, g is the magnitude of the gyromagnetic ratio of the ^{3}He nucleus. Equations (3) and (4) differ from Eqs. (1) and (2) by the term proportional to $g B_{\rm rf}\omega_{\rm rf}$ as a result of the symmetry violation. It plays a role of the energy gap or "an effective mass." A detailed derivation of the oscillation modes of the HPD-SD structure affected by the symmetry breaking field $B_{\rm rf}$ is presented in the Appendix.

III. EXPERIMENT

Surface oscillation modes and torsion oscillation modes were studied in two different experiments using slightly different experimental cells[17,18] mounted on the top of a copper diffusion welded nuclear stage.[19] In both experiments, the HPD was formed and maintained by means of a continuous high-frequency field $B_{\rm rf}$ generated by the rf coil of Helmholtz type at the resonance frequency of 462 kHz in the upper part of the particular experimental cell. The bottom part of both cells served for the ^{3}He temperature measurements by means of the Pt NMR thermometer, tuning forks, and vibrating wires. Temperature scale was calibrated against the temperature of ^{3}He superfluid transition at given pressure. Once the HPD was formed, the size of the HPD inside of the cell, i.e., the position of the domain wall, was controlled (and adjusted) by the magnitude of $\mathbf{B}_0$ at a constant value of the field gradient generated by a gradient coil. Both superconducting magnets,

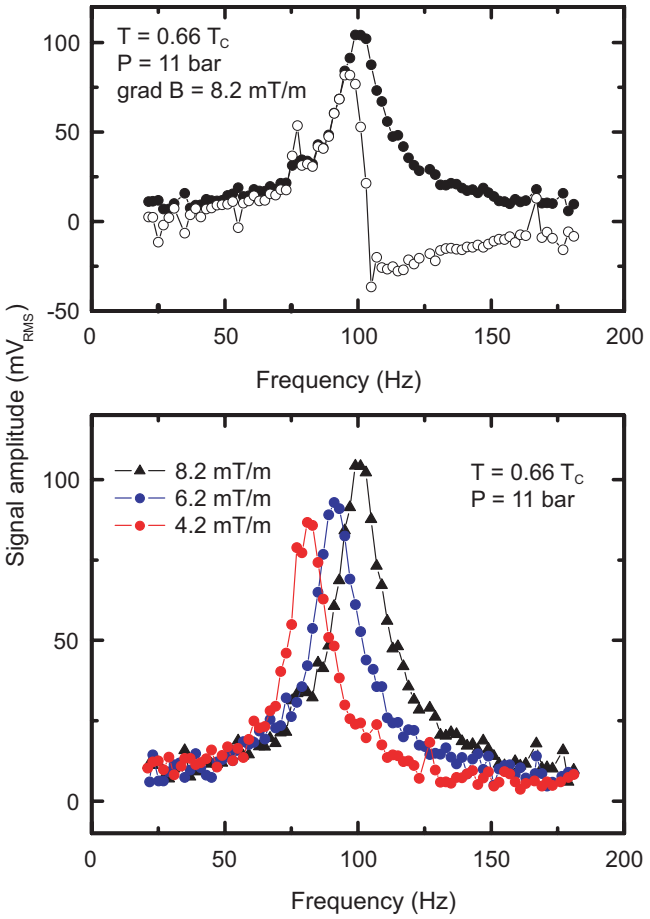

FIG. 2. (Color online) Top: absorption and dispersion resonance characteristics of the surface oscillation mode excited on the background of the dynamical equilibrium state of the magnon condensate as measured by the detection technique. Bottom: the resonance characteristics of the surface modes as a function of the field gradient.

homogeneous and gradient, were supplied from two separate constant current sources. In order to avoid the influence of the horizontal walls of the cell on the surface oscillation modes, in this case, the domain-wall position was kept in the middle of the cell.

The deflection of the HPD-SD structure from the steady state was provided by the application of an additional alternating magnetic field with an axial symmetry generated by the small longitudinal coil of the Helmholtz type. To excite a particular oscillation mode (axial or torsion), the frequency of the additional field was swept in a suitable frequency range. The response of the HPD-SD structure was detected using the demodulation technique based on the application of a high-frequency detector and a low-frequency filter, which together with a low-frequency lock-in detection allowed us to measure almost a pure low-frequency resonance signal. The reference signal for the low-frequency lock-in amplifier was taken from the generator providing the longitudinal magnetic field. The field constant of the small longitudinal coil was determined from the measurements of the position of the cw-NMR peak in the ^{3}He normal phase for various excitations of the longitudinal coil.

IV. EXPERIMENTAL RESULTS

The real homogeneously precessing domain is a spatially finite object. The effect of this spatial finiteness is that the excitation's wave vector can take on only a certain set of discrete values. As a result, the oscillations superposed on the HPD-SD structure reveal themselves as standing waves (normal modes). The surface oscillation modes were studied in a hydrodynamic regime at the pressure of 11 bar. The measurement technique allowed us to detect nearly ideal resonance characteristics of the excited surface oscillation mode (see Fig. 2). Figure 2 confirms that the measured resonance characteristics correspond to the surface modes as their resonance frequencies depend on the magnetic field gradient. Figure 3 presents the dependence of the measured resonance frequencies on the field gradient. In Fig. 3, two theoretical dependencies are shown as well, for the first ($\xi_{0,1} = 3.8317$) and the second ($\xi_{0,2} = 7.0156$) axial modes as they were calculated according to Fomin's expression (2) for a freely precessing two-domain structure:

$$\Omega^2 = \frac{1}{2\sqrt{2}} \frac{\nabla\omega_L}{\omega_L} \sqrt{\left(5c_T^2 - c_L^2\right)\left(5c_L^2 + 3c_T^2\right)} \frac{\xi_{m,i}}{R}. \qquad (5)$$

Because the HPD is encircled by an impenetrable cell wall, the k_T in expressions (2), (3), and (4) can take on only the values that satisfy the condition $\partial J_m(k_T R)/\partial(k_T R) = 0$, which implies that $k_T = \xi_{m,i}/R$, where $\xi_{m,i}$, are zeros of the first derivative of the Bessel function of the order of m ($m = 0,1,2,\ldots$) and R is the radius of the domain wall assumed to be the same as the radius of the experimental cell.

Obviously, there is a discrepancy between the theoretical prediction and experimental results. Relying on Fomin's theory, we interpreted this difference as a consequence of the domain-wall thickness.[17] The theory neglects the wall thickness, however, in reality it grows as the field gradient decreases as

$$\lambda_F = \left(\frac{c_L^2}{\omega_L \nabla\omega}\right)^{1/3}. \qquad (6)$$

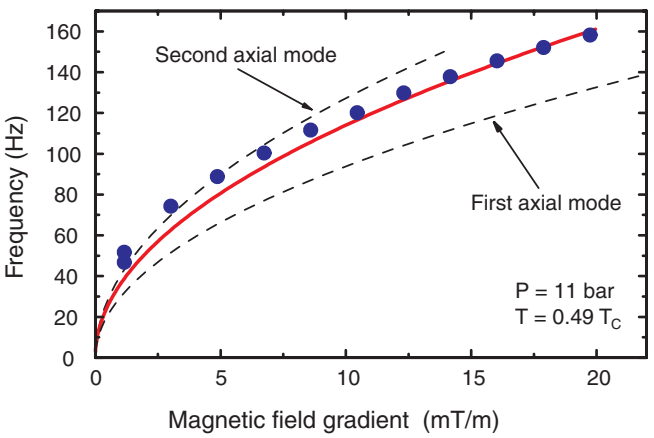

FIG. 3. (Color online) Resonance frequencies of the axial surface mode as a function of the field gradient measured at the temperature of 0.49 T_C and pressure of 11 bar. Black dashed lines correspond to the theoretical calculations according to Fomin's theory for the first and the second axial modes, while the red line corresponds to the theoretical model presented.

Then, the finite domain-wall thickness together with the effect of magnetic nonwetting[20,21] cause that real radius R of the oscillating domain wall [see expression (5)] is not the same as the cell radius, but it corresponds to an effective radius. This interpretation was partially correct and partially wrong.

As it follows from the theoretical calculations presented in the Appendix, the presence of the high-frequency excitation field $B_{\rm rf}$ violates the U(1) symmetry of the HPD precession. Due to this, the dispersion relation is lifted by an additional frequency shift proportional to the rf-field amplitude $B_{\rm rf}$. Assuming that the position of the domain wall is in the middle of the sufficiently long cell, the frequency of the first axial mode ($k_T = \xi_{0,1}/R = 3.8317/R$) can be expressed as

$$\Omega^2 = \frac{3}{4}\frac{g\nabla B}{\omega_{\rm rf}}\sqrt{\frac{2}{3}\left(5c_T^2 - c_L^2\right)} \times \sqrt{\frac{4}{\sqrt{15}} g B_{\rm rf}\omega_{\rm rf} + \frac{5c_L^2 + 3c_T^2}{3}\frac{(3.8317)^2}{R^2}}. \quad (7)$$

In expression (7), there are no free parameters that could be used to adjust theoretical data to the experimental ones. The line in Fig. 3 represents the dependence calculated by using Eq. (7) ($B_{\rm rf} = 2\mu T$, $R = 3$ mm). As it can be seen from Fig. 3, there is a reasonable agreement between the experimental data and the theoretical prediction for higher-field gradients, but there is a discrepancy for lower-field gradients. The domain wall becomes thinner for higher gradients and the experimental reality satisfies better the premises of the theoretical model. This is not true for the low-field gradients, where one needs to take into account the thickness of the domain wall itself [see expression (6)] and, as it was already mentioned above, consider an effective radius of the domain wall. Data shown in Fig. 3 we reckoned for an indirect confirmation of our theoretical model. In order to make a proper proof of this model, one needs to realize these measurements at the constant field gradient and with the constant domain-wall position, and to measure the dependence of the resonance frequency of the excited axial mode on the rf-field amplitude $B_{\rm rf}$ directly.

Measurements of the torsion oscillation mode using the cw-NMR technique were performed at the pressure of 0 bar.[18] The torsion mode is related to the oscillations of the phase of precession of the precessing spins in the bulk of the HPD and its resonance frequency depends on the HPD length (see below). The presence of the $\mathbf{B}_{\rm rf}$ defines a preference orientation for the spin density. This field again breaks the U(1) symmetry of the homogeneously precessing domain with respect to the phase of precession. A torsion Goldstone mode acquires an energy gap as a direct consequence of this symmetry violation and becomes a non-Goldstone mode. As the boundary conditions are the cell wall at one end and the domain wall at the other end of HPD, the frequency of the fundamental mode ($k_T = \xi_{0,0}/R = 0, k_L = \pi/2L$) can be expressed as

$$\Omega^2 = \frac{3\Omega_B^2}{8\Omega_B^2 + 3\omega_{\rm rf}^2}\left(\frac{4}{\sqrt{15}} g B_{\rm rf}\omega_{\rm rf} + \frac{\left(5c_T^2 - c_L^2\right)\pi^2}{6L^2}\right), \quad (8)$$

where L is the HPD length.

Figure 4 shows the dependence of the resonance frequencies squared on the rf-field amplitude $B_{\rm rf}$. The line represents the fit to experimental data using Eq. (8). The fit does not cross zero

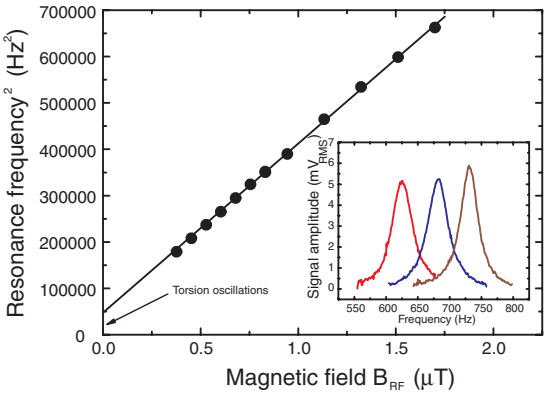

FIG. 4. (Color online) Resonance frequencies squared of the torsion mode of the HPD as the function of the $B_{\rm rf}$ amplitude measured at the temperature of 510 μK and pressure of 0 bar. The line is the fit to experimental data using Eq. (8). Inset shows the resonance characteristics measured for three rf-field excitations demonstrating the frequency shift with $B_{\rm rf}$ amplitude.

at zero rf-field amplitude, and this nonzero value corresponds to the frequency of the free torsion mode, i.e., the second term in expression (8).

Figure 5 shows the resonance frequencies as a function of the HPD length. The line is the fit to experimental data using Eq. (8). The inset to Fig. 5 presents the resonance characteristics of the excited torsion modes measured at three different lengths of the HPD. As the HPD becomes shorter, the resonance frequency rises up, however, the oscillation mode simultaneously becomes more dissipative reducing thus the amplitude of its oscillations. As it was shown in Ref. 18, there are two main processes of the energy dissipation: (i) the spin diffusion and (ii) the Leggett-Takagi mechanism. The dissipation rate by the spin diffusion depends on the HPD length as $1/L^2$, while this via the Leggett-Takagi mechanism is linear with HPD length L. Therefore, the dissipation by the

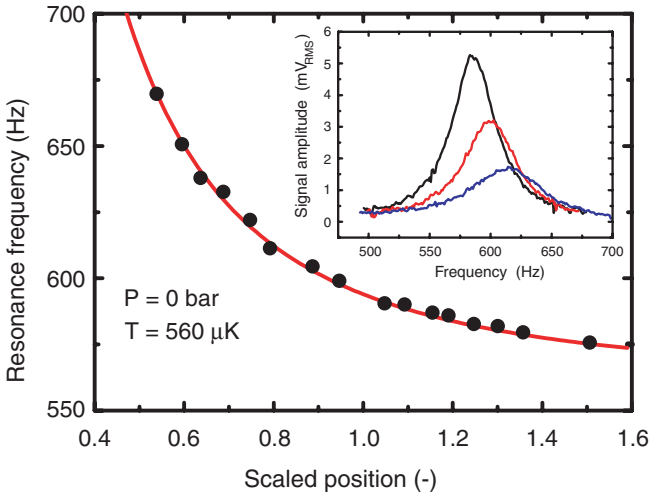

FIG. 5. (Color online) Resonance frequency of the torsion mode as a function of the HPD length scaled by the cell length. The line is the fit to experimental data using Eq. (8). Inset shows the resonance characteristics measured for three various HPD lengths at the constant amplitude of $B_{\rm rf}$.

spin diffusion dominates when the length of the HPD becomes shorter.

If the HPD fills up the whole cell (so there is no SD present and therefore no domain wall), the collective mode [see Eq. (8)] transforms to its long-wavelength limit with $1/L \to 0$. This describes uniform oscillations of magnetization on the background of HPD, i.e., the NMR in the rotating frame of reference. In fact, the high-frequency field $B_{\rm rf}$ is static in the frame of reference rotating at frequency $\omega_{\rm rf}$ and therefore may play the same role as the static magnetic field B does in a laboratory frame: it aligns magnetization with the field direction. An additional longitudinal field, which is invariant to the rotation, applied on this system at a proper frequency may deflect this magnetization creating NMR in a rotating frame of reference.

V. CONCLUSION

We presented the theoretical model supported by the experimental data showing that the presence of the high-frequency magnetic field $\mathbf{B}_{\rm rf}$ breaks the U(1) symmetry of the Bose-Einstein condensate of magnons in superfluid ^{3}He-B formed as a homogeneously precessing domain and, as a consequence of this symmetry violation, the Goldstone oscillation modes of this system, which are gapless in the absence of rf field, become non-Goldstone in the presence of this field, as they acquire the energy gap or "mass."

ACKNOWLEDGMENTS

The Centre of Low Temperature Physics is operated as the Centre of Excellence CFNT MVEP of the Slovak Academy of Sciences. We acknowledge support from the Microkelvin, the project of 7. FP of EU, APVV-0515-10 (former project APVV-0432-07), VEGA-0128, CEX-Extrem SF of EU (ITMS 26220120005). We wish to acknowledge support from M. Človečko and E. Gažo and technical support from Š. Bicák and G. Pristáš. Support provided by the US Steel Košice s.r.o. is also very appreciated.

APPENDIX

Low-frequency oscillations of a spin density superposed on its homogeneous precession are investigated. In measurements, the HPD in ^{3}He-B is formed and maintained by the cw-NMR method. To model such a situation, the components of the field along the Cartesian axes are chosen in the form $B_x = -B_{\rm rf}\cos\omega_{\rm rf}t$, $B_y = B_{\rm rf}\sin\omega_{\rm rf}t$, and $B_z = -B + z\nabla B$. The spin motion is coupled with that of the order parameter. In ^{3}He-B, the order parameter is the rotation matrix that transforms the orbital coordinates to the spin ones.

In what follows, it is assumed that the orbital reference frame is fixed in space and that the rotation of the spin reference frame frame starts from the Balian-Werthamer ^{3}P$_0$ state. It is convenient to describe this rotation by means of the Euler angles $\alpha(x,y,z,t)$, $\beta(x,y,z,t)$, and $\gamma(x,y,z,t)$ (or better $\Phi = \alpha + \gamma$). The action of fields α, β, and Φ reads as

$$S = \int_{t_1}^{t_2} dt \int_{(V)} \mathcal{L}\, dx\, dy\, dz, \tag{A1}$$

where the Lagrangian density is given by the relation

$$\mathcal{L} = \frac{\chi_B}{g^2}(\epsilon_{\rm kin} - \epsilon_{\rm grad} - \epsilon_{\rm dip}). \tag{A2}$$

Here, g is the magnitude of the gyromagnetic ratio of ^{3}He nucleus, χ_B is the magnetic susceptibility per unit volume of ^{3}He-B, and[22–25]

$$\begin{aligned}\epsilon_{\rm kin} = {} & (1-\cos\beta)\alpha_t^2 - (1-\cos\beta)\,\alpha_t\Phi_t + \tfrac{1}{2}\Phi_t^2 + \tfrac{1}{2}\beta_t^2 \\ & + g(B - z\nabla B)[(1-\cos\beta)\alpha_t + (\cos\beta)\Phi_t] \\ & + gB_{\rm rf}[(\Phi_t - \alpha_t)\sin\beta\cos(\omega_{\rm rf}t + \alpha) \\ & - \beta_t \sin(\omega_{\rm rf}t + \alpha)],\end{aligned} \tag{A3}$$

$$\begin{aligned}\epsilon_{\rm grad} = {} & \tfrac{1}{2}\left[c_L^2(1-\cos\beta)^2 + c_T^2(1-\cos^2\beta)\right]\left(\alpha_x^2 + \alpha_y^2\right) \\ & + \left[c_L^2(1-\cos\beta)\cos\beta + c_T^2(1-\cos\beta)^2\right]\alpha_z^2 \\ & - c_L^2(1-\cos\beta)(\alpha_x\Phi_x + \alpha_y\Phi_y) \\ & - \left(2c_T^2 - c_L^2\right)(1-\cos\beta)\alpha_z\Phi_z \\ & + \tfrac{1}{2}c_L^2\left(\Phi_x^2 + \Phi_y^2\right) + \tfrac{1}{2}\left(2c_T^2 - c_L^2\right)\Phi_z^2 \\ & + \tfrac{1}{2}c_T^2\left(\beta_x^2 + \beta_y^2\right) + \tfrac{1}{2}c_L^2\beta_z^2,\end{aligned} \tag{A4}$$

$$\epsilon_{\rm dip} = \tfrac{2}{15}\,\Omega_B^2\left[(1+\cos\beta)(1+\cos\Phi) - \tfrac{3}{2}\right]^2. \tag{A5}$$

The part of local spin density that is induced by the order-parameter motion is given by

$$s_x = \frac{\chi_B}{g^2}[(\Phi_t - \alpha_t)\sin\beta\cos\alpha - \beta_t\sin\alpha], \tag{A6}$$

$$s_y = \frac{\chi_B}{g^2}[(\Phi_t - \alpha_t)\sin\beta\sin\alpha + \beta_t\cos\alpha], \tag{A7}$$

$$s_z = \frac{\chi_B}{g^2}[(\Phi_t - \alpha_t)\cos\beta + \alpha_t]. \tag{A8}$$

Here, $\alpha_t = \partial\alpha/\partial t$, $\alpha_x = \partial\alpha/\partial x$, $\alpha_y = \partial\alpha/\partial y$, $\alpha_z = \partial\alpha/\partial z$, etc. Quantities c_L and c_T are velocities of two kinds of the spin waves. Ω_B is the Leggett frequency of the longitudinal resonance in the ^{3}He-B. In the density of gradient energy $\epsilon_{\rm grad}$, the high-frequency oscillations due to the overall precession are integrated out.

Using the calculus of variations to find an extremum of the action (A1) leads to the Euler-Lagrange equations for α, β, and Φ:

$$\begin{aligned}\frac{\delta S}{\delta\alpha(x,y,z,t)} \equiv {} & \frac{\partial}{\partial t}\frac{\partial\mathcal{L}}{\partial\alpha_t} + \frac{\partial}{\partial x}\frac{\partial\mathcal{L}}{\partial\alpha_x} + \frac{\partial}{\partial y}\frac{\partial\mathcal{L}}{\partial\alpha_y} \\ & + \frac{\partial}{\partial z}\frac{\partial\mathcal{L}}{\partial\alpha_z} - \frac{\partial\mathcal{L}}{\partial\alpha} = 0, \text{ etc.}\end{aligned} \tag{A9}$$

The solutions of these equations extremize the action (A1).

As in the pulsed NMR case,[12] the steady-state solution of the equations of motion is expected to describe a two-domain structure. In one domain, the spins point along the positive z direction and are at rest, while in the other, the spins are deflected off the positive z direction, and all undergo precession around the z axis throughout the entire volume with the same frequency and precisely in phase. The angle of deflection β slightly exceeds 104° and varies in such a way that the dipole-dipole frequency shift compensates for the spatial variation of the Larmor frequency $gB_z(z)$.

Well inside the homogeneously precessing domain, the fields α, β, and Φ are expected to be of the form

$$\alpha_{\mathrm{HPD}} = -\omega_{\mathrm{rf}} t, \tag{A10}$$

$$\beta_{\mathrm{HPD}} = \arccos(-1/4) + (z - z_{104})\nabla\beta, \tag{A11}$$

$$\Phi_{\mathrm{HPD}} = 0. \tag{A12}$$

The point z_{104} is determined by the condition $\cos\beta = -1/4$.

Fields α_{HPD}, β_{HPD}, and Φ_{HPD} satisfy the equations of motion if z_{104} and $\nabla\beta$ fulfill the following conditions:

$$g\left(B + \frac{1}{\sqrt{15}}\,B_{\mathrm{rf}} - z_{104}\nabla B\right) - \omega_{\mathrm{rf}} = 0 \tag{A13}$$

and

$$\nabla\beta = \frac{\sqrt{15}}{4}\frac{g\omega_{\mathrm{rf}}\nabla B}{\Omega_B^2}. \tag{A14}$$

Equations describing a low-frequency oscillation superposed on the HPD are derived by using the standard procedure of linearization of the equations of motion with respect to small deviations a, b, and f of the fields α, β, and Φ from their values α_{HPD}, β_{HPD}, and Φ_{HPD}. After linearization and minor algebraic manipulation, the equations become

$$\frac{\partial^2 a}{\partial t^2} - \frac{1}{8}\left(5c_L^2 + 3c_T^2\right)\left(\frac{\partial^2 a}{\partial x^2} + \frac{\partial^2 a}{\partial y^2}\right) - \frac{1}{4}\left(5c_T^2 - c_L^2\right)\frac{\partial^2 a}{\partial z^2} - \frac{3}{8}\left(5c_T^2 - 3c_L^2\right)\frac{\omega_{\mathrm{rf}} g\nabla B}{\Omega_B^2}\frac{\partial a}{\partial z} + \frac{\sqrt{15}}{10}\omega_{\mathrm{rf}} g B_{\mathrm{rf}} a - \frac{\sqrt{15}}{10}\omega_{\mathrm{rf}}\frac{\partial b}{\partial t}$$
$$- \frac{1}{2}\frac{\partial^2 f}{\partial t^2} + \frac{1}{2}c_L^2\left(\frac{\partial^2 f}{\partial x^2} + \frac{\partial^2 f}{\partial y^2}\right) + \frac{1}{2}\left(2c_T^2 - c_L^2\right)\frac{\partial^2 f}{\partial z^2} + \frac{3}{8}\left(2c_T^2 - c_L^2\right)\frac{\omega_{\mathrm{rf}} g\nabla B}{\Omega_B^2}\frac{\partial f}{\partial z} = 0, \tag{A15}$$

$$\frac{\partial^2 b}{\partial t^2} - c_T^2\left(\frac{\partial^2 b}{\partial x^2} + \frac{\partial^2 b}{\partial y^2}\right) - c_L^2\frac{\partial^2 b}{\partial z^2} + \Omega_B^2 b + \frac{\sqrt{15}\omega_{\mathrm{rf}}}{4}\frac{\partial a}{\partial t} - \frac{\sqrt{15}}{4}(z - z_{104}) g\nabla B\frac{\partial f}{\partial t} = 0, \tag{A16}$$

$$\frac{\partial^2 f}{\partial t^2} - c_L^2\left(\frac{\partial^2 f}{\partial x^2} + \frac{\partial^2 f}{\partial y^2}\right) - \left(2c_T^2 - c_L^2\right)\frac{\partial^2 f}{\partial z^2} + \frac{3}{8}(z - z_{104}) g\omega_{\mathrm{rf}}\nabla B f + \frac{\sqrt{15}}{4}(z - z_{104})\, g\nabla B\,\frac{\partial b}{\partial t} - \frac{5}{4}\frac{\partial^2 a}{\partial t^2}$$
$$+ \frac{5}{4}c_L^2\left(\frac{\partial^2 a}{\partial x^2} + \frac{\partial^2 a}{\partial y^2}\right) + \frac{5}{4}\left(2c_T^2 - c_L^2\right)\frac{\partial^2 a}{\partial z^2} + \frac{15}{16}\left(2c_T^2 - c_L^2\right)\frac{g\omega_{\mathrm{rf}}\nabla B}{\Omega_B^2}\frac{\partial a}{\partial z} = 0. \tag{A17}$$

The actual HPD has the length L and is formed in a cylindrical cell of diameter R. The superposed oscillations thus reveal themselves as standing waves (the normal modes). The normal modes can be found only if the boundary conditions are known.

The spin current can not penetrate into the walls of the experimental cell. As the spin current is related to gradients in the spin part of the order parameter, the normal derivatives of a, b, or f must vanish at the side cell's walls. At the top of the cell, the following condition must be satisfied:

$$\left[\left(5c_T^2 - c_L^2\right)\frac{\partial a}{\partial z} + 2\left(c_L^2 - 2c_T^2\right)\frac{\partial f}{\partial z}\right]_{z=z_{104}+L} = 0. \tag{A18}$$

The condition at the domain wall is different. The wavelength of the low-frequency oscillations is comparable to the longitudinal and transverse dimensions of the domain and is larger than the thickness of the domain wall. Therefore, it may be assumed that (i) the set of points defined by the condition $\cos\beta = -1/4$ transforms from a plane into a very slightly bent surface, and (ii) the domain wall is infinitely thin.

If the plane undergoes a really small deflection, only the out-of-plane displacements of its points are relevant. That is, the displacement vector for the plane's points is $u_x = u_y = 0$, $u_z = u(x,y,t)$. Taking a line integral of $\delta S/\delta\alpha$ along a line parallel to the z axis, from z_1 to z_2 via $z_{104} + u$, assuming the domain wall as infinitely thin, and letting z_2 tend to $z_{104} + u$, the following relation is obtained:

$$\left[\frac{\partial\mathcal{L}}{\partial\alpha_z} - \frac{\partial\mathcal{L}}{\partial\alpha_t}\frac{\partial u}{\partial t}\right]_{z=z_{104}+u+0} = 0. \tag{A19}$$

Assuming that a spin pattern in an infinitesimal vicinity of a point (x,y,z_{104}) displaces as a "solid structure," another relation is obtained:

$$\left[\frac{\partial b}{\partial t} + \frac{\partial u}{\partial t}\nabla\beta\right]_{z=z_{104}+0} = 0. \tag{A20}$$

Combining these two, the required condition at the domain wall is found, which in the linear order of smallness reads as

$$\left[\Omega_B^2\frac{\partial b}{\partial t} + \left(\frac{\sqrt{15}}{8}\, g\nabla B\right)\left[\left(5c_T^2 - c_L^2\right)\frac{\partial a}{\partial z} + 2\left(c_L^2 - 2c_T^2\right)\frac{\partial f}{\partial z}\right]\right]_{z=z_{104}+0} = 0. \tag{A21}$$

A frequency window for the low-frequency oscillations is assumed to be within frequency range $c\nabla\beta \ll \omega \ll \Omega_B$, where c denotes the spin-wave velocity. In this case, Eq. (A16) provides

$$b = -\frac{\sqrt{15}}{4\,\Omega_B^2}\left[\omega_{\mathrm{rf}}\frac{\partial a}{\partial t} - (z - z_{104})\, g\nabla B\frac{\partial f}{\partial t}\right]. \tag{A22}$$

Substituting this to Eq. (A17) and allowing that $\Omega_B < \omega_{\rm rf}$, it follows that $f/a \ll 1$. Due to this, variable f may be omitted in Eq. (A17) and in the boundary conditions if they appear together with a. As a result, the following wave equation has to be solved:

$$\left(\frac{8}{3}+\frac{\omega_{\rm rf}^2}{\Omega_B^2}\right)\frac{\partial^2 a}{\partial t^2}-\frac{1}{3}\left(5c_L^2+3c_T^2\right)\left(\frac{\partial^2 a}{\partial x^2}+\frac{\partial^2 a}{\partial y^2}\right) -\frac{2}{3}\left(5c_T^2-c_L^2\right)\frac{\partial^2 a}{\partial z^2}+\frac{4}{\sqrt{15}}\,g\omega_{\rm rf}B_{\rm rf}\,a\;=\;0, \quad \text{(A23)}$$

and a solution must satisfy the boundary conditions

$$\left[\frac{\partial^2 a}{\partial t^2}-\frac{g\nabla B}{2\omega_{\rm rf}}\left(5c_T^2-c_L^2\right)\frac{\partial a}{\partial z}\right]_{z=z_{104}}=0, \qquad \left[\frac{\partial a}{\partial z}\right]_{z=z_{104}+L}=0, \qquad \left[\frac{\partial a}{\partial r}\right]_{r=R}=0. \quad \text{(A24)}$$

Here, r is the first of the cylindrical coordinates (r,φ,z). The two-domain structure (HPD) formed in the cell can have a bulk and surface oscillation modes.

The surface modes concentrate near the domain wall. A general solution that meets these requirements can be written in the form

$$a=\left[a_1 J_m(k_T r)+a_2 N_m(k_T r)\right]\cos m(\varphi-a_3) \times \cosh(k_L z+a_4)\cos(\omega t+a_5), \quad \text{(A25)}$$

where $m=0,1,2,3,\ldots$, J_m is the Bessel function of the order m, and N_m is the Neumann function of the order m.

The solution (A25) must be finite everywhere in the HPD, it must satisfy the equations of motion throughout the HPD, and fulfill the boundary conditions on the HPD surface. Allowing for all these factors provides a group of modes which are characterized by a negligible amplitude of b relative to those of a, and by characteristic frequencies that are the solutions of the equation

$$\omega^2=\frac{3}{4}\frac{g\nabla B}{\omega_{\rm rf}}\,\omega'\sqrt{\frac{2}{3}\left(5c_T^2-c_L^2\right)}\tanh\left(\frac{L}{\sqrt{\frac{2}{3}\left(5c_T^2-c_L^2\right)}}\,\omega'\right), \quad \text{(A26)}$$

where

$$\omega'=\left[\frac{4}{\sqrt{15}}\,\omega_{\rm rf}g\,B_{\rm rf}+\frac{1}{3}\left(5c_L^2+3c_T^2\right)\left(\frac{\xi_{m,i}}{R}\right)^2-\frac{8\Omega_B^2+3\omega_{RF}^2}{3\Omega_B^2}\,\omega^2\right]^{1/2}. \quad \text{(A27)}$$

In this equation, $\xi_{m,i}$, are zeros of the derivative of the Bessel function [i.e., the roots of the equation $\partial J_m(\xi)/\partial\xi=0$].

For very low frequencies, Eq. (A26) simplifies to the form

$$\omega^2=\frac{3}{4}\frac{g\nabla B}{\omega_{\rm rf}}\sqrt{\frac{2\left(5c_T^2-c_L^2\right)}{3}} \times\sqrt{\frac{4}{\sqrt{15}}\omega_{\rm rf}g\,B_{\rm rf}+\frac{5c_L^2+3c_T^2}{3}\left(\frac{\xi_{m,i}}{R}\right)^2} \times\tanh Q(L,B_{\rm rf},\xi_{m,i}), \quad \text{(A28)}$$

where $Q(L,B_{\rm rf},\xi_{m,i})$ is expressed as

$$Q(L,B_{\rm rf},\xi_{m,i})=\frac{L\sqrt{\frac{4}{\sqrt{15}}\,\omega_{\rm rf}g\,B_{\rm rf}+\frac{5c_L^2+3c_T^2}{3}\left(\frac{\xi_{m,i}}{R}\right)^2}}{\sqrt{\frac{2}{3}\left(5c_T^2-c_L^2\right)}}. \quad \text{(A29)}$$

The bulk modes spread over the whole HPD. The corresponding solution can be written in the form

$$a=\left[a_1 J_m(k_T r)+a_2 N_m(k_T r)\right]\cos m(\varphi-a_3) \times\cos(k_L z+a_4)\cos(\omega t+a_5). \quad \text{(A30)}$$

For the actual bulk normal modes, the frequencies are the solutions of the equation

$$\omega^2=\frac{3\Omega_B^2}{8\Omega_B^2+3\omega_{\rm rf}^2}\left[\frac{4}{\sqrt{15}}\,\omega_{\rm rf}g\,B_{\rm rf}+\frac{1}{3}\left(5c_L^2+3c_T^2\right)\left(\frac{\xi_{m,i}}{R}\right)^2+\frac{2}{3}\left(5c_T^2-c_L^2\right)\left[\frac{(2n+1)\frac{\pi}{2}+\varphi'}{L}\right]^2\right], \quad \text{(A31)}$$

where

$$\tan\varphi'=\frac{3}{4}\frac{g\nabla B}{\omega^2\omega_{\rm rf}}\sqrt{\frac{2}{3}\left(5c_T^2-c_L^2\right)}\sqrt{\frac{8\Omega_B^2+3\omega_{\rm rf}^2}{3\Omega_B^2}\,\omega^2-\frac{1}{3}\left(5c_L^2+3c_T^2\right)\left(\frac{\xi_{m,i}}{R}\right)^2-\frac{4}{\sqrt{15}}\,\omega_{\rm rf}g\,B_{\rm rf}}. \quad \text{(A32)}$$

Here, $n=0,1,2,\ldots$. For not very low frequencies, Eq. (A31) simplifies to the form

$$\omega^2=\frac{3\Omega_B^2}{8\Omega_B^2+3\omega_{\rm rf}^2}\left[\frac{4}{\sqrt{15}}\,\omega_{\rm rf}g\,B_{\rm rf}+\frac{1}{3}\left(5c_L^2+3c_T^2\right)\left(\frac{\xi_{m,i}}{R}\right)^2+\frac{2}{3}\left(5c_T^2-c_L^2\right)\left[\frac{(2n+1)\frac{\pi}{2}}{L}\right]^2\right]. \quad \text{(A33)}$$

It is worth to note that the torsion mode we refer to in our article corresponds to the fundamental mode characterized by $\xi_{0,0}=0$ and $n=0$.

*skyba@saske.sk

[1] D. Snoke, Nature (London) **443**, 403 (2006).
[2] L. V. Butov, C. W. Lai, A. Z. Ivanov *et al.*, Nature (London) **417**, 47 (2002).
[3] J. Kasprzak, M. Richard, S. Kundermann *et al.*, Nature (London) **443**, 409 (2006).
[4] S. O. Demokritov, V. E. Demidov, O. Dzyapko *et al.*, Nature (London) **443**, 430 (2006).
[5] Yu. M. Bunkov, E. M. Alakshin, R. R. Gazizulin *et al.*, JETP Lett. **94**, 68 (2011) [Pisma v Zh. Eksp. Teor. Fiz. **94**, 68 (2011)].
[6] Yu. M. Bunkov and G. E. Volovik, Phys. Rev. Lett. **98**, 265302 (2007).
[7] Yu. M. Bunkov and G. E. Volovik, J. Low Temp. Phys. **150**, 135 (2008).
[8] V. V. Dmitriev, I. V. Kosarev, M. Krusius, D. V. Ponarin, V. M. H. Ruutu, and G. E. Volovik, Phys. Rev. Lett. **78**, 86 (1997).
[9] D. J. Cousins, S. N. Fisher, A. I. Gregory, G. R. Pickett, and N. S. Shaw, Phys. Rev. Lett. **82**, 4484 (1999).
[10] I. A. Fomin, Sov. Phys.–JETP **61**, 1207 (1985) [Zh. Eksp. Teor. Fiz. **88**, 2039 (1985)].
[11] I. A. Fomin, JETP Lett. **43**, 171 (1986) [Pisma Zh. Eksp. Teor. Fiz. **43**, 134 (1986)].
[12] I. A. Fomin, in *Helium Three*, edited by W. P. Halperin and L. P. Pitaevskii (Elsevier, Amsterdam, 1990), p. 609.
[13] Yu. M. Bunkov *et al.*, JETP Lett. **43**, 168 (1986) [Pisma Zh. Eksp. Teor. Fiz. **43**, 131 (1986)].
[14] Yu. M. Bunkov, V. V. Dmitriev, and Yu. M. Mukharskii, Phys. B (Amsterdam) **178**, 196 (1992).
[15] V. V. Dmitriev *et al.*, J. Low Temp. Phys. **138**, 765 (2005).
[16] Ľ. Lokner, A. Feher, M. Kupka, R. Harakály *et al.*, Europhys. Lett. **40**, 539 (1997).
[17] E. Gažo, M. Kupka, M. Medeová, and P. Skyba, Phys. Rev. Lett. **91**, 055301 (2003).
[18] M. Človečko, E. Gažo, M. Kupka, and P. Skyba, Phys. Rev. Lett. **100**, 155301 (2008).
[19] P. Skyba, J. Nyéki, E. Gažo *et al.*, Cryogenics **37**, 293 (1997).
[20] Yu. M. Bunkov, O. D. Timofeevskaya, and G. E. Volovik, Phys. Rev. Lett. **73**, 1817 (1994).
[21] P. Skyba, R. Harakály, Ľ. Lokner, and A. Feher, Phys. Rev. Lett. **75**, 477 (1995).
[22] K. Maki, Phys. Rev. B **11**, 4264 (1975).
[23] K. Maki and H. Ebisawa, Phys. Rev. B **13**, 2924 (1976).
[24] V. P. Mineev and G. E. Volovik, J. Low Temp. Phys. **89**, 823 (1992).
[25] T. S. Misirpashaev and G. E. Volovik, J. Low Temp. Phys. **89**, 885 (1992).